Food Science of Animal Products

Research Article

High pressure homogenization induced egg yolk low-density lipoprotein remodeling and its application in loaded paprika oleoresin

Di Xiao[1,§], Gan Hu[1,2,§], Xuan Yao[3], Beibei Wang[1,2], Jinqiu Wang[1] ✉, Fang Geng[1]

[1] *Key Laboratory of Coarse Cereal Processing (Ministry of Agriculture and Rural Affairs), School of Food and Biological Engineering, Chengdu University, Chengdu 610106, China*
[2] *Institute for Advanced Study, Chengdu University, Chengdu 610106, China*
[3] *College of Food Science and Technology, Huazhong Agricultural University, Wuhan 430070, China*
[§] These authors contributed equally to this article.
✉ Address correspondence to Jinqiu Wang, wangjinqiu@cdu.edu.cn

Received: June 26, 2024; Revised: July 13, 2024; Accepted: July 18, 2024

Abstract: Paprika oleoresin (PO) is extensively utilized as a natural pigment in the food industry. However, its application in aqueous phase foods is hindered by due to its lipophilicity and sensitivity to oxygen, heat, and light. This study developed an aqueous PO solution using low-density lipoprotein (LDL) as a carrier, which was remodeled through high pressure homogenization treatment (0–100 MPa). Comprehensive analyses were conducted to characterize the micro-morphology, particle size, potential, and encapsulation efficiency (EE) of the solution, alongside evaluations of its storage, thermal, and ultraviolet (UV) irradiation stability, in addition to physicochemical and structural characterization of the remodeled LDL. The results showed that after high pressure homogenization (100 MPa, 10 cycles) treatment, the delamination of LDL-PO solution was significantly reduced, the average particle size decreased by 37.2%, the EE increased by 9.2%, and the storage, thermal, and UV irradiation stability increased from 30.83%, 64.42%, and 77.56% to 62.90%, 76.97%, and 92.98%, respectively. In addition, sodium dodecylsulfate-polyacrylamide gel electrophoresis (SDS-PAGE) and fluorescence spectroscopy analyses revealed that high pressure homogenization treatment enhanced the interaction and binding between LDL and PO, thus significantly improved the solubility and stability of PO in water. In this study, an aqueous solution of PO with higher stability and embedding rate was obtained by the greener and safer high pressure homogenization technique, offering new avenues for PO application in the food industry and innovative uses of LDL as a carrier for bioactive substances.

Keywords: egg yolk low-density lipoprotein; high pressure homogenization; paprika oleoresin

Citation: D. Xiao, G. Hu, X. Yao, et al., High pressure homogenization induced egg yolk low-density lipoprotein remodeling and its application in loaded paprika oleoresin, Food Sci. Anim. Prod. 2 (2024) 9240064. https://doi.org/10.26599/FSAP.2024.9240064.

1 Introduction

Paprika oleoresin (PO) is a natural pigment extracted from the ripe chili peppers and is widely used in the food industry as a natural source of carotenoid pigments[1]. PO not only has excellent coloring ability, but also has significant biological activities such as antioxidant, anti-inflammatory, and anticancer functions due to its carotenoid content[2–3]. However, PO is sensitive to environmental conditions such as oxygen, heat, and light, which can easily lead to the loss of its functional activity[4]. In addition, the lipophilic nature of PO results in poor water solubility, greatly limiting its utilization in food. To address these issues, improving the water dispersibility and stability of PO has become a hot research topic in recent years[5].

Oil-in-water emulsions and nanoemulsions containing carotenoids in the dispersed oil phase are promising delivery systems to improve their bioavailability. Some studies have utilized surfactants with different hydrophilic-lipophilic balances to prepare nanoemulsions of PO, and the results showed a decrease in the rate of degradation and an increase in the stability of the emulsions[6].

Liposomes are small closed vesicles spontaneously formed by amphiphilic molecules in aqueous solution, capable of encapsulating hydrophilic, lipophilic, or amphiphilic active substances, and are widely used in food, pharmaceutical, and cosmetic fields[7–8]. Due to their small particle size, large surface area, and high mass transfer efficiency, nanoliposomes can significantly improve the bioavailability of encapsulated active substances.

The low-density lipoprotein (LDL) in egg yolk, 17–60 nm in diameter, features a "core-shell" structure: triglycerides and cholesterol form the lipid "core" of LDL, and a phospholipid monolayer forms the "shell" around this lipid core, where proteins are distributed. This structure is highly similar to that of liposomes, making LDL an ideal carrier for the delivery of fat-soluble active ingredients. However, the key challenge lies in how to effectively load PO into the natural structure of LDL.

In our previous study, LDL remodeling was induced by an ultrasound-assisted pH-shifting technique to achieve aqueous phase dissolution of PO[9]. Our study[10] further confirmed that this pH-shifting remodeled the molecular structure of LDL and hydrolyzed the lipids in LDL into fatty acid sodium salts under alkaline conditions, leading to a decrease in particle size and an

increase in specific surface area. This property provides an important prerequisite for LDL to load active ingredients. Ultrasonication effectively promotes the interaction between reconstituted LDL and fat-soluble components, thereby improving the storage stability of these components. However, the pH-shifting method requires the use of strong alkali treatment, posing environmental concerns. Additionally, the crushing and thermal effects of ultrasonic treatment can destabilize or even destroy the liposome structure, leading to leakage of the contents. Therefore, finding greener solutions is particularly important.

High pressure homogenization (HPH), as a commonly used crushing emulsification preparation method for emulsion delivery system, can avoid the use of a large number of irritating organic solvents in order to obtain liposome suspensions with small average particle size, uniform distribution and good stability. The HPH treatment mainly achieves a strong refining effect on liposomes through the impact, shear and cavitation between materials under high-pressure conditions, and the thermal effect of its treatment process is not obvious[11]. The study of Tang et al.[12] showed better thermal and storage stability by encapsulating VC in nanoliposomes through primary emulsification and HPH. Meanwhile, HPH treatment has been shown to reduce particle size reduction due to pressure gradient forces and can produce particles from molecules with small and uniform particle size distribution[13]. In a study, whey protein nanoparticles loaded with coenzyme Q_{10} were prepared by HPH, enhancing their antioxidant properties and bioavailability through improved hydrogen bonding and hydrophobic interactions, and optimizing particle size and electronegativity for better encapsulation efficiency (EE). The dual action of HPH, which promotes the interaction of proteins with other constituents and the reduction of the particle size, makes it a versatile method for the fabrication of new nanoparticles as a generalized method.

Based on this, our study aimed to induce LDL remodeling through HPH and construct stable aqueous phase solutions of PO. Firstly, the effect of LDL encapsulating PO after HPH treatment was clarified, and then the storage, thermal, and ultraviolet (UV) stability of PO aqueous solution were evaluated, and then the characterization and mechanism of HPH-reconstituted LDL were investigated. Reconstructing LDL and loading PO via HPH can substantially expand the application of PO in food processing.

2 Materials and methods

2.1 Materials and reagent

PO was sponsored by Lucky Huaguan Graphics Co. All reagents used in the experiments were AR grade and purchased from China Pharmaceutical Group Corporation (Sinopharm Holdings). Filter membrane (polyethersulfone (PES), 0.45 μm, 25 mm) was purchased from Discovery Platform; 5 × loading buffer (P0015L), BeyoGel™ Plus PAGE gel, and staining solution were purchased from Shanghai Biyuntian Biotechnology Co. Fresh eggs from Roche laying hens (40–50 weeks of age, caged, standard feeding) were provided by Sichuan Shengdilacun Eco-Foods Co., Ltd. (Mianyang, Sichuan). Egg yolk LDL was extracted according to the method described by Wang et al.[14] and Xie et al.[15].

2.2 Preparation of LDL-PO aqueous system

The pH of the phosphate buffered saline (PBS; 10 mmol/L, original pH 7.2) system was adjusted to pH 12 by adding NaOH (2 mol/L), PO was added to the PBS system, and then the system was magnetically stirred at 800 r/min for 45 min to prepare a system with a PO concentration of 10 mg/mL, and then the pH was adjusted to 9, and the aqueous system that formed was called PBS-PO.

To the aqueous PBS-PO system (PO, 10 mg/mL), 10 mg/mL LDL was added, and the prepared system was named LDL-PO, and then this system was pre-sheared using a high-speed disperser (8 000 r/min, 5 min, Ningbo Xinzhi Biotech Co.).

2.3 Preparation of sample with HPH treatment

HPH treatment was performed using an ultra-high-pressure homogenizer (SCIENTZ-207, Ningbo Xinzhi Biotech Co.). The LDL-PO system was homogenized for 10 cycles (8 min)[16] at 0, 25, 50, 75, and 100 MPa, respectively. Samples were recorded as L-P-CK (0 MPa), L-P-H25 (25 MPa), L-P-H50 (50 MPa), L-P-H75 (75 MPa), and L-P-H100 (100 MPa), respectively. The LDL (10 mg/mL, PBS) was all pre-sheared (8 000 r/min, 5 min), and the LDL were similarly homogenized for 10 cycles at the above 5 different pressures, and the samples were recorded as L-CK, L-H25, L-H50, L-H75, and L-H100, respectively.

2.4 Determination of floating rate (FR)

L-P-CK, L-P-H25, L-P-H50, L-P-H75, and L-P-H100 (15 mL) were placed in vials (20 mL, φ = 27.5 mm) and stored at room temperature in the dark for 48 h. FR was determined using the following formula:

$$\mathrm{FR}\ (\%) = \frac{H}{H_0} \times 100 \tag{1}$$

Where H is the height (mm) of the undissolved upper layer, and H_0 is the total height (mm) of the system, H and H_0 are measured with vernier calipers.

2.5 Determination of EE

The PO encapsulation rate of high pressure homogenized LDL-PO nanocapsules was determined by the perovskite method. The system to be tested was diluted with anhydrous ethanol, and 5 mL of the system to be tested was taken for periplasm (PES, 0.45 μm, 25 mm), and the absorbance of PO before and after periplasm was measured at 460 nm with anhydrous ethanol as the reference. After substituting into the standard curve to determine the concentration of PO, the EE was calculated using the following formula:

$$\mathrm{EE}\ (\%) = \frac{C_{\mathrm{total}} - C_{\mathrm{free}}}{C_{\mathrm{total}}} \times 100 \tag{2}$$

Where C_{total} is the total concentration (mg/mL) of PO in the system and C_{free} is the concentration (mg/mL) of free PO in the system.

2.6 Determination of turbidity

Zero-turbidity water (distilled water passed through a 0.2 μm membrane) was prepared to calibrate the instrument, after which the samples were diluted 10-fold and measured directly with a turbidimeter (WZS-188; Shanghai Yidian Scientific Instrument Co., Ltd.).

2.7 Analysis of dynamic light scattering (DLS)

The prepared samples were diluted to 0.01 mg/mL with deionized water. ζ-Potential and average particle size of each group of samples

were measured using a nanoparticle sizer (ZS90, Malvern Zetasizer Nano, Malvern, UK). Measurements were made at 25 °C and scanned automatically by the machine. Three replicate measurements were performed for each sample.

2.8 Analysis of sodium dodecylsulfate-polyacrylamide gel electrophoresis (SDS-PAGE)

The samples (80 μL) were mixed directly with 5 × loading buffer (20 μL), and the mixtures were processed in a boiling water bath for 10 min, cooled to room temperature, and then the samples (10 μL) were loaded individually into each lane of the BeyoGel™ Plus PAGE gel. Then electrophoresis was performed at 150 V for 50 min, and protein molecular weight was determined using pre-stained protein markers. The gel was stained with staining solution for 25–35 min, and then destained by multiple gel rinses with deionized water until the rinses were colorless and the gel background was clear.

2.9 Analysis of storage stability, thermal stability and UV stability of HPH-reconstituted LDL-PO

L-P-CK, L-P-H25, L-P-H50, L-P-H75, and L-P-H100 (15 mL) were placed in vials (20 mL, φ = 27.5 mm) and stored at room temperature for 28 d. The color value (CV) of the samples were determined on days 1, 3, 5, 7 and 9. The sample was weighed in a colorimetric tube (10 mL) and the absorbance was determined using a UV-Vis spectrophotometer (UV1901PC, Shanghai Aoan Scientific Instruments, Shanghai, China). CV was calculated according to the following equation:

$$\mathrm{CV} = \frac{A \times f \times 166.7}{m \times 100} \tag{3}$$

Where A is the absorbance of the diluted sample at 460 nm; f is the dilution ratio; m is the weight (g) of the sample.

L-P-CK, L-P-H25, L-P-H50, L-P-H75, and L-P-H100 (1 mL) were added to the vials (2 mL, φ = 11.6 mm) and heated at 60 °C for 6, 12, 18, and 24 h.

L-P-CK, L-P-H25, L-P-H50, L-P-H75, and L-P-H100 (0.5 mL) were added to a 24-well plate (inner diameter of the cuvette was 10 mm, thickness of the sample system was about 3 mm) and irradiated with UV light (6 W, irradiation distance of 40 cm) for 2, 4, 6, and 8 h.

CV retention rate (%) was calculated using the CVs of the irradiated samples compared to the initial values.

2.10 Determination of fluorescence spectra

A fluorescence spectrophotometer (FL-970; Shanghai Tianmei Scientific Instrument Co., Ltd.) was used to detect the protein chromophores of the HPH-treated LDL-PO-modified system. The excitation slit width and emission slit width were both 2.5 nm, and the excitation wavelength was 280 nm. The scanned emission wavelengths were 300–500 nm.

2.11 Observation of confocal laser scanning microscope (CLSM)

L-P-CK, L-P-H25, L-P-H50, L-P-H75, and L-P-H100 samples were selected for further observation of their morphology using a Leica stellaris 5 CLSM (Leica Microsystems, Germany). LDL was stained with rhodamine B (green fluorescence). Measurements were made using excitation wavelengths: 580 nm for rhodamine B using an argon/krypton laser and 462 nm for PO using a helium/neon laser.

2.12 Observation of scanning electron microscope (SEM)

The samples (L-CK, L-H25, L-H50, L-H75, and L-H100) were diluted to 0.05 mg/mL with deionized water of the corresponding pH. The diluted samples (10 μL) were added to clean slides, air-dried for 24 h, sprayed with gold, and observed and recorded with a SEM with an accelerating voltage of 10 kV.

2.13 Determination of Fourier transform infrared (FTIR) spectra

After freeze-drying the LDL samples for 36 h to form a powder using a freeze-dryer (LC-12N-80, Shanghai Li-Chen Instrument Technology Co., Shanghai, China), the lyophilized powder (1–2 mg) was taken and mixed thoroughly with dried KBr (100 mg), placed on a plate with ZnSe crystals and pressed into a tablet. Using an attenuated total reflection-FTIR spectrometer (Nicolet Is5, Thermo Fisher Scientific Ltd., USA), FTIR were obtained by 32 scans with a resolution of 4 cm^{-1} at wave numbers of 400–4 000 cm^{-1}[17].

2.14 Data analysis

Data were means ± standard deviations. One-way analysis of variance (ANOVA) was performed using Prism 8 (GraphPad, La Jolla, CA, USA) and $P < 0.05$ was considered significant.

3 Results and discussion

3.1 Physicochemical properties of HPH-reconstituted LDL

The particle size of LDL is a critical parameter that influences its physical and chemical stability under different environmental conditions and also significantly affects the EE, absorption, and release of bioactive components[18]. The turbidity and particle size of the L-CK system (10 mg/mL, pH 7.2) were 288.1 NTU and (69.19 ± 0.55) nm, respectively (Figure 1A), and the particle size of LDL gradually decreased with increasing homogenization pressure. When the homogenization pressure was 25 MPa, the average particle size of LDL increased to (80.40 ± 2.30) nm (Figure 1B), and the turbidity also increased to 296.83 NTU, and the system became turbid, indicating that at this time, LDL was prone to the phenomenon of sphere structure fragmentation and then fusion and aggregation, resulting in the generation of larger nano-aggregates. When the pressure was 100 MPa, compared with L-CK, the turbidity decreased significantly to 105.43 NTU ($P < 0.05$), the system became clarified, and the average particle size decreased to (62.87 ± 1.25) nm.

These changes may be attributed to the fact that under higher homogenizing pressure and the strong shear and cavitation forces in the microchannels caused LDL to disperse into smaller and more homogeneous particles, and the structure of LDL was dissociated and de-folded, and the particle size decreased[19]. The transparency of the LDL system increased with the increase of homogenization pressure, which was related to the decrease of the average particle size with homogenization pressure, and the consequent decrease of the light scattering phenomenon of large particles in the suspension[20].

The larger the absolute value of the ζ-potential is, the stronger the electrostatic interactions between the protein molecules and the more stable the system will be[21]. ζ-Potential of the L-CK system was (−12.57 ± 0.81) mV, and the ζ-potential of LDL increased to (−10.90 ± 0.72) at 25 MPa (Figure 1C). As the pressure continued to rise, the absolute value of the ζ-potential of the LDL system continued to strengthen, with the contrary trend as the change of

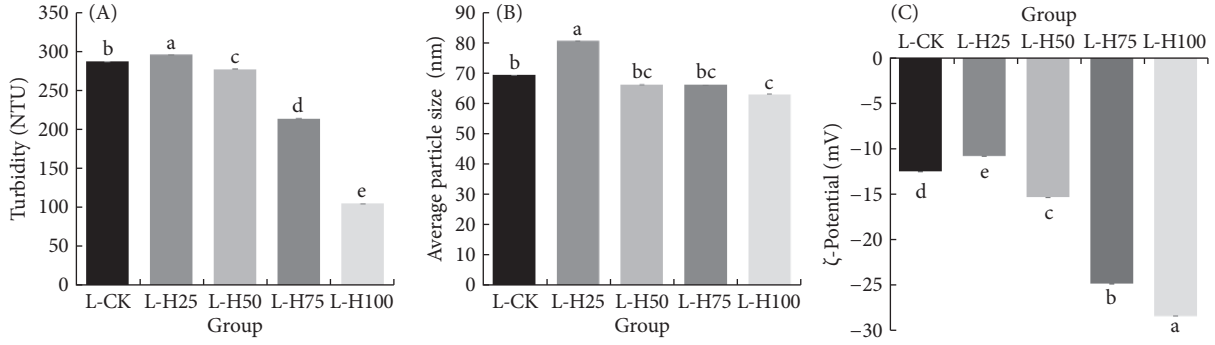

Figure 1 Comparison of physicochemical properties of low-density lipoprotein (LDL) under different homogenization pressure treatments. (A) Turbidity; (B) Average particle size; (C) ζ-Potential. Different letters (a–e) indicate significant differences ($P < 0.05$).

the particle size and turbidity, and the ζ-potential was (–28.37 ± 1.40) mV when the pressure increased by 100 MPa, which could be attributed to the change of the internal structure of protein molecules under the HPH, causing the protein molecules to unfold and the interaction of non-covalent bonding between protein molecules made the negatively charged groups of the protein more exposed on the surface of protein molecules, which increased the number of surface charges of the protein. The increase in the absolute value of the ζ-potential led to stronger electrostatic repulsion, which may be one of the reasons for the greater stability of the LDL system after HPH treatment. The results showed that the HPH treatment improved the stability of the LDL system mainly by reducing the particle size of LDL and increasing the surface potential of LDL. These changes suggested that the HPH treatment induced LDL molecular remodeling.

3.2 Structural characteristics of HPH-reconstituted LDL

3.2.1 SDS-PAGE analysis

The molecular structure of LDL samples was further analyzed to reveal the mechanism of the effect of HPH treatment on the functional and structural properties of LDL. The protein subunit composition of LDL samples was analyzed by SDS-PAGE (Figure 2A). The protein fraction of LDL consists of hydrolyzed fragments (apolipoproteins) of the precursor protein apolipoprotein B

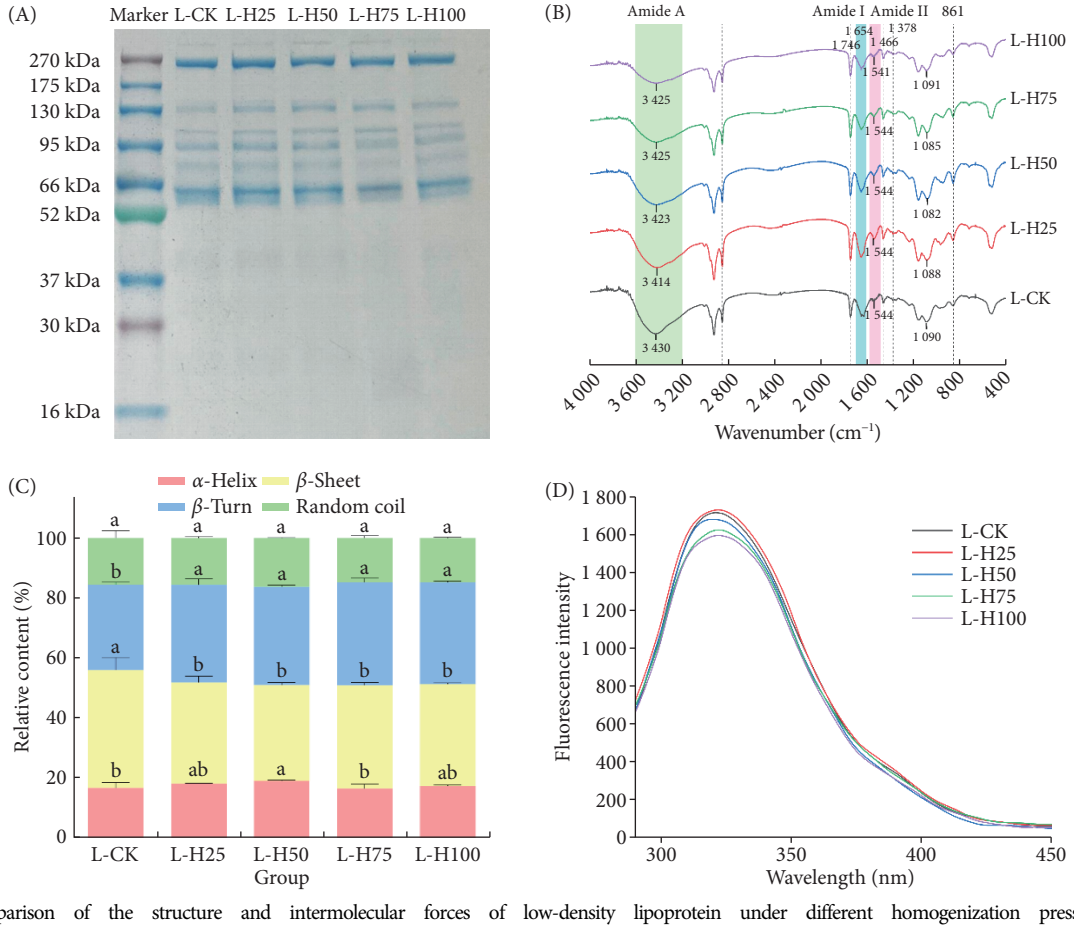

Figure 2 Comparison of the structure and intermolecular forces of low-density lipoprotein under different homogenization pressure treatments. (A) Electrophoretic profile; (B) FTIR spectra; (C) Distribution of secondary structural forms; (D) Fluorescence profile. Different letters (a–b) indicate significant differences ($P < 0.05$).

(APOB). Previous studies on the composition of LDL have shown that LDL electrophoretic profiles indicate that LDL consists of 7–9 major apolipoproteins of different molecular weights[22]. In the present study, the protein profiles did not change significantly in band intensity and number with increasing homogenization pressure, indicating that covalent peptide bonds were not broken, suggesting that HPH treatment did not alter the subunit species and composition of LDL. A similar trend was reported for HPH studies, such as hawksbill protein[23] and quinoa protein[24], in which HPH also did not cause disruption of protein molecules. That is, the study suggested that HPH treatment did not alter the protein composition and primary structure of LDL.

3.2.2 FTIR spectra analysis

To further investigate the conformational changes of LDL before and after HPH treatment, the secondary structure of LDL was analyzed by FTIR spectra. The amide I region (1 700–1 600 cm^{-1}) consists of C=O (70%–85%) and C–N stretching vibrations (10%–20%) and is the most sensitive band to changes in the secondary structure of proteins[25]. The FTIR spectra of L-CK and high-pressure homogenized LDL had identical absorption peaks at 1 653–1 658, 2 852–2 854, and 2 922–2 925 cm^{-1} (Figure 2B), which corresponded to the amide I band (the protein fraction of LDL), the symmetric stretching vibration of the $-CH_2$ group, and the asymmetric stretching vibration, respectively[26]. All LDL samples showed absorption peaks in the characteristic spectral bands. The characteristic peaks in the amide A and amide II bands were shifted to different degrees with the increase of pressure: the characteristic peaks in the amide A band gradually shifted from 3 430 to 3 425 cm^{-1} at 100 MPa; the characteristic peaks in the amide II band also shifted by 3 cm^{-1} (from 1 544 to 1 541 cm^{-1}), at which time, the strength of the hydrogen bond was altered, which led to the depolymerization of the molecules, indicating that the molecular structure of LDL was gradually unfolding. In the FTIR spectra of LDL, the absorption peaks of C=O stretching vibration at 1 746 cm^{-1} and the double absorption peaks of C–O–C stretching vibration at 1 090 and 1 150 cm^{-1} are the characteristic absorption peaks of the ester (lipid fraction of LDL). The characteristic absorption peaks at 1 090 cm^{-1} were red-shifted with the increase of pressure, which was caused by the formation of hydrogen bonding of the C=O bond of the ester (25–75 MPa), and blue-shift occured up to 100 MPa, when a return to higher values of the vibrational frequency of the C=O bond may occur, manifesting itself as hydrogen bond breaking.

After 100 MPa pressure treatment, the peak at 1 654 cm^{-1} became wider and smaller, which corresponded to the decrease of α-helix, probably because the hydrogen bonds in the protein molecules were destroyed during the HPH treatment process, thus affecting the stability of the α-helix. This destruction led to the disintegration of the α-helix structure, which changed its vibration pattern in the FTIR spectra. The β-sheet also decreased with increasing pressure (Figure 2C), indicating that the aggregation of the whole LDL molecules was weakened and the system was better dispersed, which was consistent with the results of particle size and turbidity studies. The results suggest that partial unfolding and rearrangement of proteins, or disruption of intramolecular ionic bonds, may have occurred in LDL molecules after HPH treatment[27]. The FTIR spectra showed that the HPH had some effect on hydrogen bonding and induced some changes in the secondary structure of LDL.

3.2.3 Fluorescence spectra analysis

The emission wavelength is 290 nm, and in a polar environment, aromatic residues of proteins (such as tryptophan and tyrosine) are exposed. Therefore, changes in the tertiary structure of proteins can be determined by changes in fluorescence intensity and wavelength shifts[28]. The effect of HPH treatment on the endogenous fluorescence intensity of LDL is shown in Figure 2D. In addition, the maximum fluorescence intensity of the untreated sample was 1 705, which rose and reached a maximum value of 1 732 at 25 MPa HPH treatment, and the maximum fluorescence intensity gradually decreased to 1 596 when the pressure was further increased (50–100 MPa). The maximum fluorescence wavelength (λ_{max}) was also blue-shifted from 323 to 321 nm at 25 MPa, suggesting that the HPH treatment changed the nonpolar environment in which the chromophore was located, promoting the unfolding of the LDL structure to expose the internal chromophore, and the maximum fluorescence intensity increased, indicating that the chromophore entered the hydrophobic environment; when the pressure exceeded 25 MPa, it caused the molecules to be partially denatured and aggregated, resulting in the chromophore being buried again, and with the increase of the treatment pressure, the intensity of the emission peak gradually decreased, and at this time, the chromophore entered the hydrophilic environment, and the particle size, the results of ζ-potential were consistent. The protein fluorescence intensity of LDL decreased after HPH treatment, the reason may be that the pressure makes the protein structure unfold, tryptophan and tyrosine residues are exposed on the surface of the molecule, which increases the enzyme recognition. This proves that HPH treatment caused the LDL-isolated egg white tertiary conformation to change[23].

3.2.4 Microscopic morphology

In order to more visually reflect the remodeling effect of HPH treatment on LDL, SEM images of LDL treated with different HPH conditions were taken separately. The SEM images showed that LDL molecules without HPH treatment were spheres and appeared extensive protein aggregates in the size range of 50–200 nm (Figure 3), and the observed results were in agreement with the results of the previously determined average particle size. As observed on SEM images, L-CK images showed many irregular shapes and extensive adhesion/aggregation, and with increasing pressure, especially at higher pressures (100 MPa), a large number of protein aggregates were greatly disaggregated into smaller particles of uniform size. However, after treatment with higher intensity pressure (100 MPa), the particles were uniform in appearance (50–100 nm), the spherical particles were intact, rounded and separated from each other, and the adhesion was significantly reduced. These morphologies were consistent with the significant reduction of L-CK particle size and turbidity, indicating that the high-intensity HPH treatment was conducive to the formation of a stable LDL system.

3.3 Stability of HPH-reconstituted LDL-PO

3.3.1 Molecular characterization

After HPH treatment, the turbidity of the LDL-PO system increased from 37.87 (L-P-CK) to 45.10 NTU (L-P-H75) with increasing pressure ($P < 0.05$), and then reduced to 43.82 NTU by a small margin after 100 MPa HPH treatment (Figure 4A). The trend

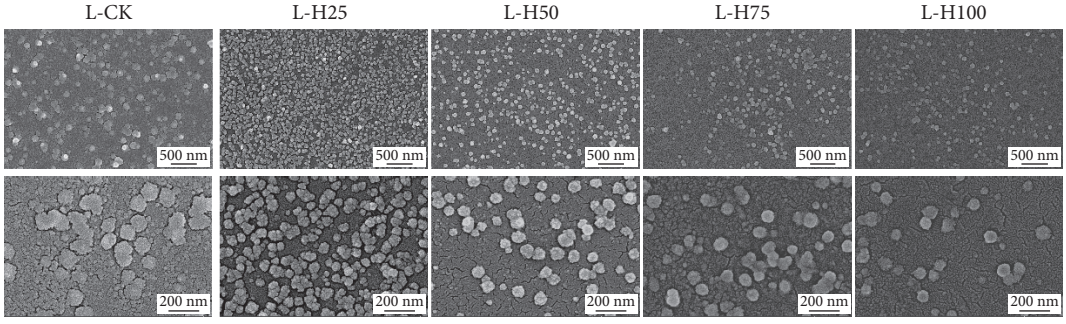

Figure 3 Scanning electron microscope image of low-density lipoprotein under different homogenization pressure treatments.

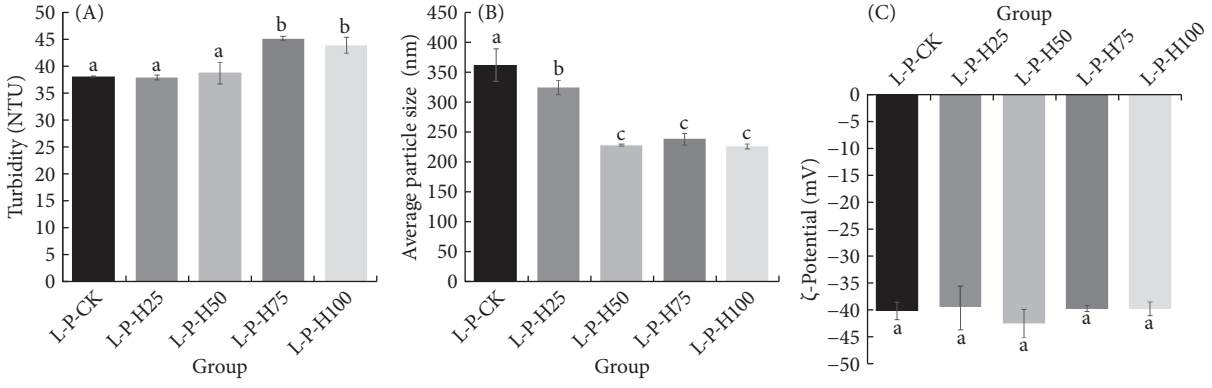

Figure 4 Comparison of physicochemical properties of low-density lipoprotein-paprika oleoresin under different homogenization pressure treatments. (A) Turbidity; (B) Average particle size; (C) ζ-Potential. Different letters (a–c) indicate significant differences ($P < 0.05$).

of average particle size change was opposite to that of turbidity, and the overall trend of particle size decreased with the increase of pressure; the particle size decreased from 362.4 to 229.1 nm at pressures from 0 to 50 MPa, increased to 239.2 nm at 75 MPa, and further decreased to 227.5 nm at 100 MPa (Figure 4B). The results showed that the HPH treatment (100 MPa) could substantially reduce the particle size of the LDL-PO system compared with the untreated group.

The ζ-potential of the L-P-CK system was –40.233 mV, which was enhanced to –42.5 mV when the pressure was increased to 50 MPa, and the electronegativity decreased with the increase of the pressure (Figure 4C). The absolute value of the ζ-potential of the LDL-PO showed a tendency of increasing and then decreasing with the increase of homogenization pressure. The pressure of 50 MPa showed the largest absolute value of ζ-potential, indicating that the HPH treatment increased the number of net charges on the surface of the molecules and improved the intermolecular electrostatic repulsion; the decrease in absolute value of ζ-potential when the pressure was further increased may be attributed to the fact that the excessively high pressure promoted the dissociative solubilization of the fatty acids in the PO, which consumed the hydroxyl groups.

The increase in turbidity of LDL-PO after HPH treatment indicated the formation of larger aggregates containing a large amount of PO, suggesting that the LDL was loaded with more PO molecules, which confirms that HPH treatment promotes the binding of LDL to PO[29]. The reason for the decrease in particle size due to LDL-PO may be that HPH promotes the binding of PO to LDL, resulting in an increase in the specific surface area of LDL and an increase in droplet stability[30–31]; this may be due to the higher shear, cavitation, and turbulence under high pressure[32], which favors protein aggregation and the formation of colloidal particles produced by protein aggregation under more homogeneous reaction conditions, which enhances the functional properties of proteins and uniform particle size distribution[33]. HPH treatment reduced the size of cannabinoid protein nano-aggregates by 3.2- and 1.9-fold, respectively[34], and increased the solubility and foaming capacity of cannabinoid proteins[35]. It was shown that the smaller the particle size of the emulsion, the higher the bioavailability of capsaicinoids[31], and the HPH treatment could further increase the bioavailability of PO. These results indicated that the HPH treatment further improved the homogeneity and stability of the LDL-PO aqueous system.

3.3.2 *Interactions between LDL and PO*

SDS-PAGE results showed that HPH treatment did not result in significant protein denaturation. However, there was a tendency for proteins (68 kDa) in LDL to shift to higher molecular weights under the enhancement of the intensity of HPH (Figure 5A), but this phenomenon was not detected in the LDL system alone, which may be related to the formation of covalent bonds between LDL and PO[31]. The formation of pigment tails observed in the low-molecular-weight region is most likely due to the binding interaction of the pigment with the LDL in the PO. The change in fluorescence intensity of the LDL system alone was consistent with that of the LDL-PO system, both at 25 MPa, the fluorescence intensity increased, and the fluorescence intensity continued to decrease as the pressure continued to increase, and fluorescence spectra confirmed the results, and LDL-PO fluorescence quenching occurred significantly with the increase of HPH intensity (Figure 5B), which may indicate that HPH treatment increases the degree of tight binding between the PO and LDL, and also suggest that the HPH treatment increases the binding capacity and affinity of LDL for PO, which is consistent with the observation that the homogenized LDL-PO system (L-P-H50–L-P-H100) has lower turbidity, smaller particle size, and lower uplift rate than the unhomogenized one.

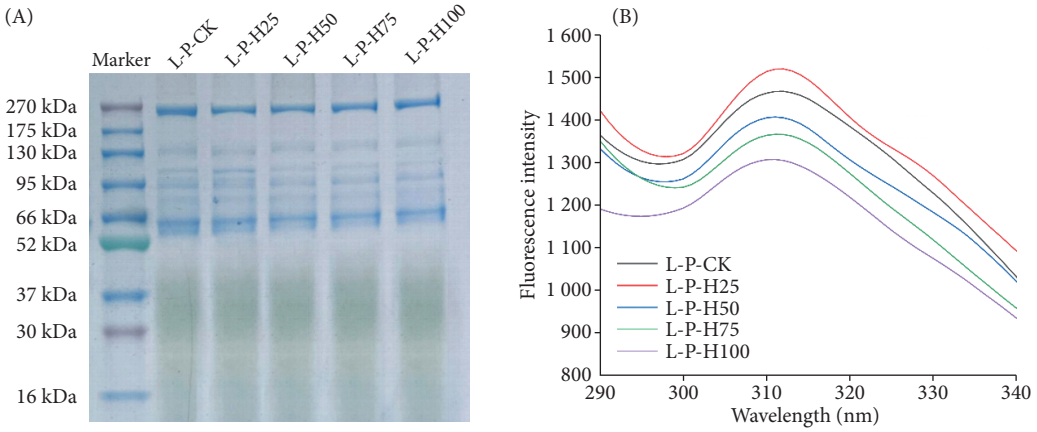

Figure 5 Comparison of the structure and intermolecular forces of low-density lipoprotein-paprika oleoresin under different homogenization pressure treatments. (A) Electrophoretic profile; (B) Fluorescence profile.

3.3.3 *Stability analysis*

HPH involves a combination of high shear, cavitation and turbulence to induce structural changes in proteins[11]. The dual action of HPH promotes protein interactions with other components and particle size reduction, making it a versatile method for fabricating new nanoparticles. The mixture of LDL and PO was treated with HPH at different pressures. The role of HPH treatment on the binding of PO to LDL was explored. The FR of the L-P-CK (0 MPa) system without HPH treatment was 4.81%, and decreased significantly ($P < 0.05$) with increasing pressure values. The FR of L-P-H100 decreased to 2.39% (Figure 6A). These results indicated that the HPH treatment could change the stability of PO in the LDL system, and the higher the pressure intensity, the better the effect of improving the uplift phenomenon in the LDL-PO system.

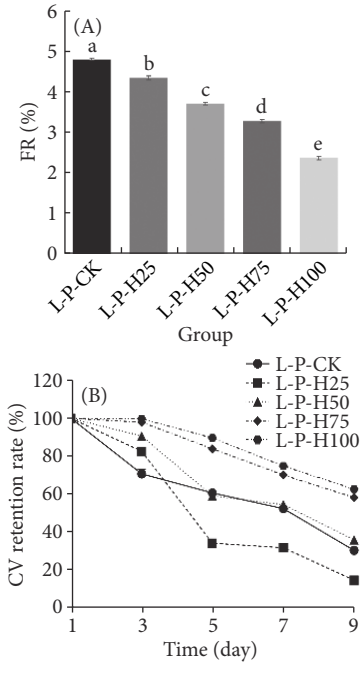

Figure 6 Comparison of the stability of low-density lipoprotein-paprika oleoresin (LDL-PO) under different homogenization pressure treatments. (A) Floating rate (FR); (B–D) Color value (CV) retention rate of LDL-PO aqueous solution under storage, thermal, and UV irradiation. Different letters (a–e) indicate significant differences ($P < 0.05$).

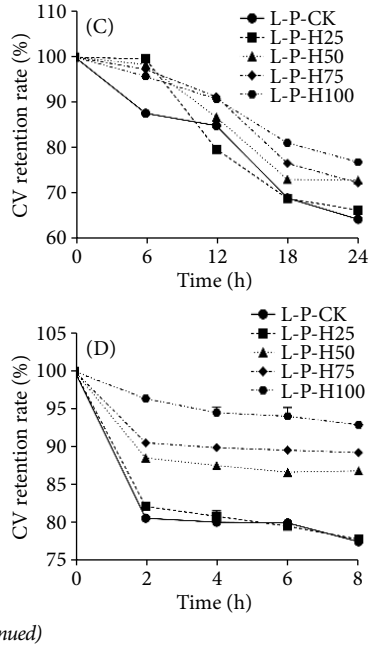

Figure 6 *(Continued)*

The effect of HPH treatment on the stability of the LDL-PO system was investigated by measuring the CV retention values of the LDL-PO system under storage, thermal, and UV irradiation conditions. The results showed that the effect of HPH treatment on stability showed a dose-effect relationship: the CV retention rates increased with increasing pressure values. For L-P-CK, the CV retention rates for storage, thermal, and UV irradiation were 30.83% (Figure 6B), 64.42% (Figure 6C) and 77.56% (Figure 6D), respectively. After HPH treatment, the CV retention rates (storage, thermal, and UV irradiation) of L-P-H100 significantly increased to 62.90%, 76.97%, and 92.98%, respectively. The results indicated that the HPH treatment promoted the interaction force between LDL and PO, which led to the full contact between LDL and PO, and ensured that the LDL-PO system maintained a well-dispersed state[36] that contributes to the stability of the whole system. Therefore, it can be concluded that the encapsulation of PO with LDL significantly improved the stability of the aqueous system, which can be attributed to the molecular level interaction between PO and the phospholipid bilayer of LDL[37]. And the HPH treatment played a crucial role in enhancing the storage, thermal, and UV irradiation stability of natural nanoliposome-LDL. In particular, the

property of PO to decompose easily under light exposure has limited the use of PO in industrial processing, so the utilization of HPH treatment can also enhance the utilization of PO in industrial production.

3.3.4 EE analysis

The EE is closely related to the degree of binding between LDL and PO, and in general, liposomal systems have inherent limitations in encapsulating water-soluble substances. Therefore, when the EE of liposomes for water-soluble substances reaches or exceeds 50%, the efficiency is considered to have reached an acceptable threshold[38]. With the increase of homogenization pressure, the EE of PO nanoliposomes reached a maximum of 84.42% (L-P-H75), and the EE decreased when the homogenization pressure reached 100 MPa ($P < 0.05$) (Figure 7). The excessive pressure may be unfavorable to the formation of the LDL-PO system and destabilize the stable structure of LDL-PO, thus reducing its encapsulation effect on PO. HPH treatment can increase the volume of the dispersed phase, reduce the particle size, and increase the molecular structure of LDL phospholipids to form double-layer spherical particles to provide more embedding space and adsorption sites for the fat-soluble active ingredient PO, which then assists in the encapsulation of PO by LDL. It can be seen that HPH further enhanced the bonding of LDL with PO and improved the stability of PO in the aqueous phase system.

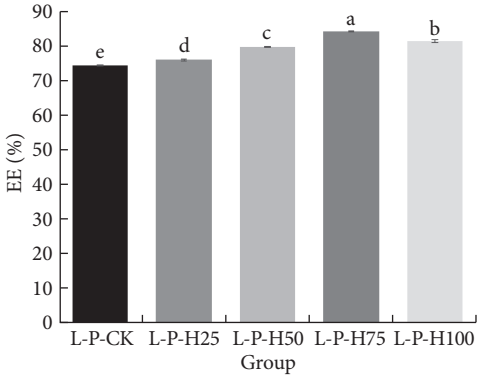

Figure 7 Comparison of encapsulation efficiency (EE) of low-density lipoprotein-paprika oleoresin under different homogenization pressure treatments. Different letters (a–e) indicate significant differences ($P < 0.05$).

3.3.5 CLSM observation

CLSM is an effective analytical method that provides useful information about the physicochemical properties of different nutrient/drug delivery systems, and the location and distribution of LDL in the LDL-PO aqueous phase system can be visualized by CLSM. Green color indicates proteins and red color indicates PO. LDL exhibited small and dense protein aggregates (green color) and was uniformly dispersed in the solution (Figure 8). Since LDL was a nanosized liposome, it was not possible to observe how LDL was loaded or embedded with PO by CLSM. However, with the increase of pressure, a denser and more uniform distribution of green fluorescent dots (proteins) could be observed. The results showed that the uniform distribution of PO in the LDL-PO aqueous system was confirmed by the CLSM, and the HPH treatment led to an increase in the dispersion of this system, representing the potential of LDL to encapsulate the active substance.

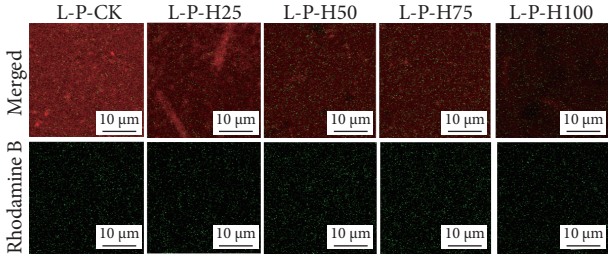

Figure 8 Confocal laser scanning microscope image of low-density lipoprotein-paprika oleoresin (LDL-PO) under different homogenization pressure treatments (× 300). Merged indicates that the fluorescence images of nile red and PO were merged. Rhodamine B indicates the fluorescence image of the sample stained with rhodamine B dye.

4 Conclusion

In this study, a stable aqueous solution of PO was successfully constructed by inducing LDL remodeling through HPH technique. The HPH treatment effectively reduced the particle size and increased the potential of LDL, and increased its surface potential and dispersion, which significantly improved the stability of the LDL system. Smaller particles and better distribution of the HPH-treated LDL solution were observed under SEM. SDS-PAGE, FTIR, and fluorescence spectroscopy analyses showed that although the primary structure of the protein of LDL was unaffected, its secondary and tertiary structures underwent rearrangement and partial unfolding. After HPH treatment, the EE of PO in LDL was significantly increased, especially up to 84.42% at 75 MPa. In addition, the HPH-treated LDL-PO system exhibited higher stability under storage, thermal, and UV irradiation conditions, indicating that the HPH treatment effectively enhanced the aqueous phase solubility and environmental stability of PO. In conclusion, the present study demonstrated that reconstitution of LDL by HPH is a green, safe, and efficient method to significantly improve the solubility and stability of PO in aqueous systems, which opens up new possibilities for the application of PO in food industry and colored food, and provides a new idea for the delivery of LDL as a fat-soluble active substance.

Conflict of interest

The author declares no conflict of interests.

Acknowledgements

This study was supported by the National Natural Science Foundation of China (32072236), and Sichuan Innovation Team Project of National Modern Agricultural Industry Technology System (SCCXTD-2024-24).

References

[1] N. de Sá Mendes, É. C. Branco de Andrade Gonçalves, The role of bioactive components found in peppers, Trends Food Sci. Technol. 99 (2020) 229–243. https://doi.org/10.1016/j.tifs.2020.02.032.

[2] N. Baenas, M. Belović, N. Ilic, et al., Industrial use of pepper (*Capsicum annum* L.) derived products: technological benefits and biological advantages, Food Chem. 274 (2019) 872–885. https://doi.org/10.1016/j.foodchem.2018.09.047.

[3] A. V. Rao, L. G. Rao, Carotenoids and human health, Pharmacol. Res. 55 (2007) 207–216. https://doi.org/10.1016/j.phrs.2007.01.012.

[4] F. R. Procopio, M. C. Ferraz, B. N. Paulino, et al., Spice oleoresins as value-added ingredient for food industry: recent advances and perspectives, Trends Food Sci. Technol. 122 (2022) 123–139. https://doi.org/10.1016/j.tifs.2022.02.010.

[5] A. Pérez-Gálvez, M. I. Mínguez-Mosquera, Degradation, under non-oxygen-mediated autooxidation, of carotenoid profile present in paprika oleoresins with lipid substrates of different fatty acid composition, J. Agr. Food Chem. 52(3) (2004) 632–637. https://doi.org/10.1021/jf0351063.

[6] L. A. Pascual-Pineda, E. Flores-Andrade, M. Jiménez-Fernández, et al., Kinetic and thermodynamic stability of paprika nanoemulsions, Int. J. Food Sci. Technol. 50(5) (2015) 1174–1181. https://doi.org/10.1111/ijfs.12750.

[7] S. Shah, V. Dhawan, R. Holm, et al., Liposomes: advancements and innovation in the manufacturing process, Adv. Drug Deliv. Rev. 154/155 (2020) 102–122. https://doi.org/10.1016/j.addr.2020.07.002.

[8] V. ĐORĐEVIĆ, A. BELŠČAK-CVITANOVIĆ, I. DRVENICA, et al., 3-Nanoscale nutrient delivery systems, in: A. M. Grumezescu (Ed.), Nutrient delivery, Academic Press, London, United Kingdom, 2017, pp. 87–139. https://doi.org/10.1016/B978-0-12-804304-2.00003-2.

[9] H. L. Ye, B. B. Wang, D. Xiao, et al., Ultrasound-assisted pH-shifting to construct a stable aqueous solution of paprika oleoresin using egg yolk low-density lipoprotein as a natural liposome-like nano-emulsifier, Ultrason. Sonochem. 98 (2023) 106477. https://doi.org/10.1016/j.ultsonch.2023.106477.

[10] H. L. Ye, J. Q. Wang, N. Wang, et al., Ultrasound-assisted pH-shifting remodels egg-yolk low-density lipoprotein to enable construction of a stable aqueous solution of vitamin D_3, Curr. Res. Food Sci. 5 (2022) 964–972. https://doi.org/10.1016/j.crfs.2022.05.013.

[11] L. Ma, A. L. Li, T. Q. Li, et al., Structure and characterization of laccase-crosslinked α-lactalbumin: impacts of high pressure homogenization pretreatment, LWT-Food Sci. Technol. 118 (2020) 108843. https://doi.org/10.1016/j.lwt.2019.108843.

[12] Y. Q. Tang, A. K. Zhou, S. D. Zhou, et al., Preparation of VC nanoliposomes by high pressure homogenization: process optimization and evaluation of efficacy, transdermal absorption, and stability, Heliyon 10(9) (2024) e29516. https://doi.org/10.1016/j.heliyon.2024.e29516.

[13] Y. Q. Zhu, X. Y. Sun, J. Ding, et al., Physicochemical and functional properties of a novel xanthan gum-lysozyme nanoparticle material prepared by high pressure homogenization, LWT-Food Sci. Technol. 143 (2021) 111136. https://doi.org/10.1016/j.lwt.2021.111136.

[14] N. Wang, Q. Xu, Y. Liu, et al., Highly efficient extraction and purification of low-density lipoprotein from hen egg yolk, Poul. Sci. 97(6) (2018) 2230–2238. https://doi.org/10.3382/ps/pey059.

[15] Y. X. Xie, J. Q. Wang, Y. N. Shi, et al., Molecular aggregation and property changes of egg yolk low-density lipoprotein induced by ethanol and high-density ultrasound, Ultrason. Sonochem. 63 (2020) 104933. https://doi.org/10.1016/j.ultsonch.2019.104933.

[16] R. Gaillard, D. Gagnon, V. Perreault, et al., Effect of ultra-high pressure homogenization on structural and techno-functional properties of egg yolk granule proteins, LWT-Food Sci. Technol. 178 (2023) 114624. https://doi.org/10.1016/j.lwt.2023.114624.

[17] X. Yu, S. S. Huang, F. Yang, et al., Effect of microwave exposure to flaxseed on the composition, structure and techno-functionality of gum polysaccharides, Food Hydrocolloid. 125 (2022) 107447. https://doi.org/10.1016/j.foodhyd.2021.107447.

[18] Y. L. Xie, H. M. Zhou, X. H. Liang, et al., Study on the morphology, particle size and thermal properties of vitamin A microencapsulated by starch octenylsucciniate, Agr. Sci. China 9(7) (2010) 1058–1064. https://doi.org/10.1016/S1671-2927(09)60190-5.

[19] J. D. Beltrán, L. Ricaurte, K. B. Estrada, et al., Effect of homogenization methods on the physical stability of nutrition grade nanoliposomes used for encapsulating high oleic palm oil, LWT-Food Sci. Technol. 118 (2020) 108801. https://doi.org/10.1016/j.lwt.2019.108801.

[20] H. W. Chen, W. P. Fang, A novel method for the microencapsulation of curcumin by high-pressure processing for enhancing the stability and preservation, Int. J. Pharm. 613 (2022) 121403. https://doi.org/10.1016/j.ijpharm.2021.121403.

[21] X. N. Sui, S. Bi, B. K. Qi, et al., Impact of ultrasonic treatment on an emulsion system stabilized with soybean protein isolate and lecithin: its emulsifying property and emulsion stability, Food Hydrocolloid. 63 (2017) 727–734. https://doi.org/10.1016/j.foodhyd.2016.10.024.

[22] P. Jolivet, C. Boulard, V. Beaumal, et al., Protein components of low-density lipoproteins purified from hen egg yolk, J. Agr. Food Chem. 54(12) (2006) 4424–4429. https://doi.org/10.1016/j.foodres.2023.11298610.1021/jf0531398.

[23] Y. Ma, J. Zhang, J. He, et al., Effects of high-pressure homogenization on the physicochemical, foaming, and emulsifying properties of chickpea protein, Food Res. Int. 170 (2023) 112986. https://doi.org/10.1016/j.foodres.2023.112986.

[24] L. Luo, L. Cheng, R. Zhang, et al., Impact of high-pressure homogenization on physico-chemical, structural, and rheological properties of quinoa protein isolates, Food Struct. 32 (2022) 100265. https://doi.org/10.1016/j.foostr.2022.100265.

[25] A. SADAT, I. J. JOYE. Peak fitting applied to Fourier transform infrared and Raman spectroscopic analysis of proteins, Appl. Sci. 10(17) (2020) 5918. http://doi.org/10.3390/app10175918.

[26] D. Krilov, M. Balarin, M. Kosović, et al., FT-IR spectroscopy of lipoproteins-a comparative study, Spectrochim. Acta A: Mol. Biomol. Spectrosc. 73(4) (2009) 701–706. https://doi.org/10.1016/j.saa.2009.03.015.

[27] J. Li, C. Wang, X. Li, et al., Effects of pH and NaCl on the physicochemical and interfacial properties of egg white/yolk, Food Biosci. 23 (2018) 115–120. https://doi.org/10.1016/j.fbio.2017.12.004.

[28] L. Liang, H. A. Tajmir-Riahi, M. Subirade, Interaction of β-lactoglobulin with resveratrol and its biological implications, Biomacromolecules 9(1) (2008) 50–56. https://doi.org/10.1021/bm700728k.

[29] H. M. Dong, L. X. Yang, Y. Dadmohammadi, et al., Investigating the synergistic effects of high-pressure homogenization and pH shifting on the formation of tryptophan-rich nanoparticles, Food Chem. 434 (2024) 137371. https://doi.org/10.1016/j.foodchem.2023.137371.

[30] G. Markman, Y. D. Livney, Maillard-conjugate based core-shell co-assemblies for nanoencapsulation of hydrophobic nutraceuticals

in clear beverages, Food Funct. 3(3) (2012) 262–270. https://doi.org/10.1039/c1fo10220f.

[31] D. J. Zhang, S. Y. Wang, M. C. Wang, et al., Stability and bioaccessibility improvement of capsorubin using bovine serum albumin-dextran-gallic acid and sodium alginate, Int. J. Biol. Macromol. 182 (2021) 1362–1370. https://doi.org/10.1016/j.ijbiomac.2021.05.033.

[32] G. V. Barbosa-Cánovas, J. J. Rodríguez, Update on nonthermal food processing technologies: pulsed electric field, high hydrostatic pressure, irradiation and ultrasound, Food Aust. 54(11) (2002) 513–520. https://doi.org/10.3390/foods11071003.

[33] X. Shen, T. Q. Fang, F. Gao, et al., Effects of ultrasound treatment on physicochemical and emulsifying properties of whey proteins pre- and post-thermal aggregation, Food Hydrocolloid. 63 (2017) 668–676. https://doi.org/10.1016/j.foodhyd.2016.10.003.

[34] G. Karabulut, R. Kapoor, O. Yemis, et al., Manothermosonication, high-pressure homogenization, and their combinations with pH-shifting improve the techno-functionality and digestibility of hemp protein, Food Hydrocolloid. 150 (2024) 109661. https://doi.org/10.1016/j.foodhyd.2023.109661.

[35] J. Yang, G. Liu, H. Zeng, et al., Effects of high pressure homogenization on faba bean protein aggregation in relation to solubility and interfacial properties, Food Hydrocolloid. 83 (2018) 275–286. https://doi.org/10.1016/j.foodhyd.2018.05.020.

[36] H. Gao, L. Ma, T. Q. Li, et al., Impact of ultrasonic power on the structure and emulsifying properties of whey protein isolate under various pH conditions, Proc. Biochem. 81 (2019) 113–122. https://doi.org/10.1016/j.procbio.2019.03.012.

[37] C. J. Kirby, C. J. Whittle, N. Rigby, et al., Stabilization of ascorbic acid by microencapsulation in liposomes, Int. J. Food Sci. Technol. 26 (1991) 437–449. https://doi.org/10.1111/j.1365–2621.1991.tb01988.x.

[38] M. A. Chaves, L. S. Ferreira, L. Baldino, et al., Current applications of liposomes for the delivery of vitamins: a systematic review, Nanomaterials 13(9) (2023) 1557. https://doi.org/10.3390/nano13091557.